PRECIPITATION IN THE MEDITERRANEAN REGION OBSERVED WITH TRMM MICROWAVE DATA

Martina Kästner and Jörg Steinwagner

German Aerospace Center, Oberpfaffenhofen, D-82234 Wessling, Germany

1. INTRODUCTION

Various climate models predict a decrease of precipitation in the future over many parts of the subtropics, particularly in the winter (Bolle, 2003). Therefore, it is essential to have not only climatological data from land but also from over the seas not covered by conventional observation networks but now be continuously monitored by low orbiting and geostationary satellites. Beneath operational retrievals of e.g. Grody (1991), Kummerow et al. (1996) or Wentz and Spencer (1998) some recent satellite rain retrievals in both the IR and the MW spectra are developed by Bauer (2001) using TMI estimates calibrated with PR, both onboard the TRMM satellite, Turk et al. (2002) using individual SSM/I and TMI overpasses to calibrate geo-IR precipitation estimates, Grose et al. (2002), Oh et al. (2002) and Kidd et al. (2003) among others.

The evaluation of passive microwave (PMW) precipitation algorithms which are directly linked to the 3-D structure of the precipitating system use measurements from different sensors on different satellites, like SSM/I on DMSP, TMI/PR on TRMM, or AMSU on NOAA. Passive MW techniques perform much better over the oceans than over land. The MW techniques are directly related to the hydrometeors through scattering and emission, but the low earth orbits and less frequent coverage hinders tracking of developing severe storms. While the daily course of precipitation is not easily obtained from TRMM data, IR-based techniques from geostationary satellites have been widely used due to the high revisit period. However, they have an inherent weakness regarding the physical relation between cloud top temperatures and underlying rain rate. Further, the rain characteristics vary with different climate regimes, hence, any developed method has to be validated against appropriate in situ measurements taken over the region of interest.

A cross-comparison of PMW and/or IR based algorithms with the Bologna local area model (BOLAM) in 0.25° lat-lon grid resolutions is performed for the Algerian flood in early November 2001. Although the validity of the results obtained is restricted to the case studies some general information could be extracted.

Corresponding author's address: Martina Kästner, DLR - DFD, Oberpfaffenhofen, D-82234 Wessling, Germany; E-Mail: martina.kaestner@dlr.de.

2. DATA

The Algerian severe weather event was used as a common case study for an inter-comparison of PMW, IR, combined MW/IR rainfall algorithms and the BOLAM model. The validation is performed for a severe weather event between 08 and 12 November 2001 on the Algerian coast and the Balearic Islands. The synoptic situation was characterised by strong surface winds and heavy rainfall. An intense upper-level trough pushed far to the south of Europe where a cut-off low developed. The METEOSAT-7 IR image (Fig. 1) shows the clouds with heavy rainfall on the Algerian coast. The rainfall started on late 9 Nov and ended the next day at about noon on 10 Nov, when 150 litres per m² within six hours were observed. Together with the cut-off low process heavy thunderstorms developed in a cyclogenesis over the Balearic Islands the next day. The precipitation was reported to be greater than 400 mm over two days, with a maximum of 68 litres per m² in six hours (Thomas et al., 2003).

Two processes intensified the convective development: 1) the cold maritime arctic air that crossed over the still 18° C warm Mediterranean Sea where it picked up moisture, destabilised, and met initially maritime subtropic air and 2) the strong surface winds blowing against the high mountains along the African coast (> 2300 m) caused intense orographic rainfall which led to the flooding disaster in Algiers with more than 750 deaths.

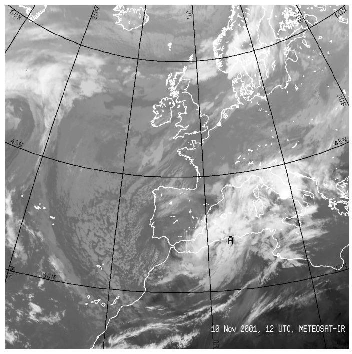

Fig. 1: METEOSAT-7 IR, 10 November 2001, 12 UTC. A = Algiers. (credit: EUMETSAT)

The input data for the used PMW algorithms (PATER, FDA) are the brightness temperatures (TB) of nine channels (10.7v,h, 19.4v,h, 21.3v, 37.0v,h, 85.5v,h GHz) with varying resolutions from 70 to 6 km from the TMI instrument onboard the low orbiting TRMM satellite. Fig. 2 shows differences of emission over water and over land for both polarizations and for different TMI channels. Over water, the rainy areas appear to be warmer than their surroundings, while over land they appear to be colder due to the high MW emission of land.

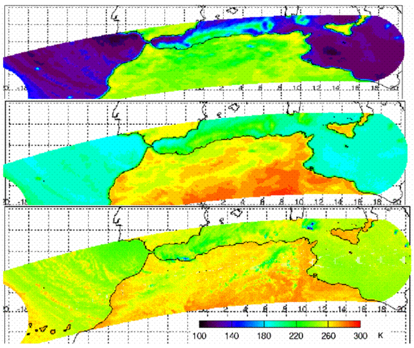

Fig. 2: TRMM TMI brightness temperatures for 19h (top), 19v (mid) and 85v (bottom) GHz channels (v = vertical, h = horizontal polarization), 10 November 2001, 00:25 UTC.

The used rain data are from 1) the BOLAM, a hydrostatic model in σ coordinates, feeded by ECMWF 6-hourly analyses (Buzzi et al., 2003), 2) the PMW satellite Frequency Difference Algorithm (FDA) of Kidd that uses the 19v and 19h GHz channels and relates their difference to the rain rate (RR), 3) the empirical Neural Rain Estimator (NRE), an operational rapid update geo-IR-based algorithm to diagnose half-hourly near-surface rainfall that uses features of the cloud top evolution and structure and information from a NWP model, 4) the Naval Research Laboratory (NRL) blended technique (Turk et al., 2002) that uses probability matching methods for dynamically-updated TB-RR lookup tables from time- and space-coincident IR and MW pixels of different satellites, and 5) the over-ocean satellite MW rainfall algorithm PATER (Bauer et al., 2001), a physical algorithm that uses only two empirical orthogonal functions instead of the nine TBs from the TMI channels basing on a database from several 3-D cloud model simulations including the melting layer. The latter algorithm has a stand-alone PMW component based on TRMM TMI (1B11) data and an optionally carefully co-located calibration part with PR (2A25) data (~5 km) downscaled to the lower TMI spatial resolution for the 10 GHz (~50 km).

3. INTER-COMPARISON OF RAIN RETRIEVALS

3.1 Method of Analysis

For the inter-comparison of several rain algorithms applied in the scope of the EURAINSAT project, continuous and categorical statistics were used within a common area extended from 15 W to 20 E and from 30 to 60 N in a common period from 09 to 11 November 2001 and with rain rates re-sampled into a 0.25° lat-lon grid (~28 km). TRMM and NRE data did not consistently cover the complete common area. The temporal coincidence was optimal for the different PMW algorithms, otherwise the temporal window was better than +/-15 min for comparisons with IR (NRL, NRE) and in most cases better than +/-90 min for comparisons with the independent model data, which have a 3-hourly temporal resolution. Comparisons were made for single orbits as well as for merged data within 3-h periods.

3.2 Results

Both PMW algorithms, PATER and FDA, rely on the same TMI orbit data and so it was expected that their comparison would result in a rather similar rainfall region and intensity. Both algorithms are assessed to be of equal quality in this heavy rainfall event, considering that the PATER algorithm is restricted to ocean surfaces and to events above 1mm/h rain intensity. The most successful comparison of PMW with other techniques was in this case the BOLAM model followed by the NRL blended MW/IR technique, both performed better than the IR technique.

Figures 3 to 7 show the RR from different retrievals for one special date (10 Nov 2001, 03 UTC).

Figure 3 shows three areas of heavy rainfall, one west of the Canary Islands, the biggest one is around Algiers, and one southeast of Sardinia. The three rain areas coincide very well with results of both MW algorithms. Even the rain intensities are similar except for the Sardinia area. FDA works over land and ocean (Fig.4), PATER exclusively over ocean. The low rain rates erroneously detected by PATER over the sea south of Sicily are attributed to strong desert aerosol also detected as aerosol fallout in Rome the next day. The rainy speckles over the Atlantic are due to cumulus convective showers within the cold air. Compared to both techniques, the BOLAM model rainfall (before nudging) shows wide agreement of the strong rain bands (Fig. 5). The rainfall intensities were rather similar; only the position of the rainfall had an error for the Sardinia area. On the other hand, the shower pattern over the Atlantic is not well matched and there are too many areas with light rain. The two IR-based algorithms, NRL and NRE (Fig. 6 and 7**),** give heavy rain areas over the Mediterranean Sea, but not at the correct position. The Algerian coast, where the maximum precipitation fell, is hardly classified as a heavy rain area. The combined MW/IR NRL algorithm shows a much better performance than the IR algorithm NRE alone.

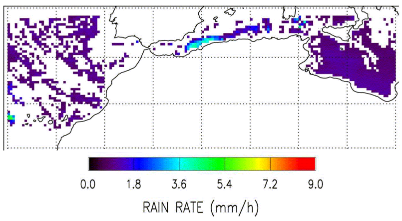

Fig. 3: PATER algorithm – MW

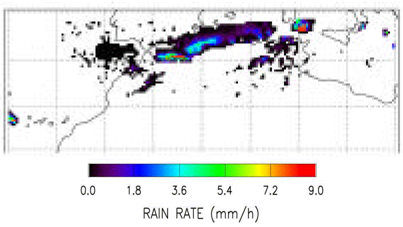

Fig. 4: FDA algorithm - PMW

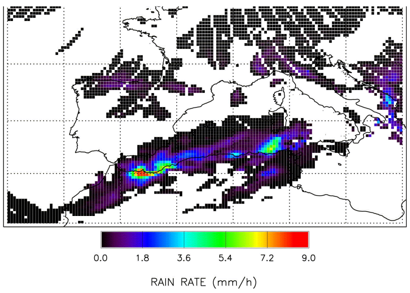

Fig. 5: BOLAM – model

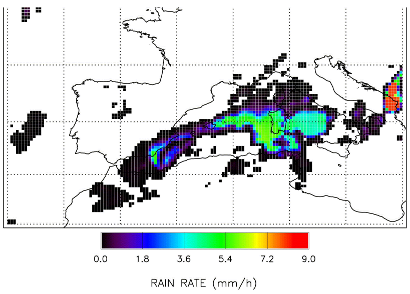

Fig. 6: NRL algorithm – combined IR-MW

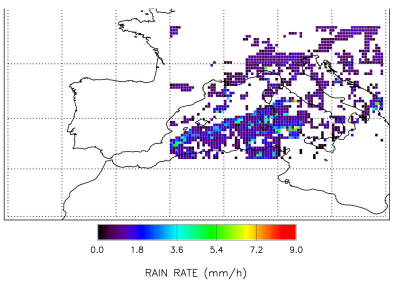

Fig. 7: NRE algorithm – IR

Overall it seems to be worthwhile to combine the high temporal resolution of IR with the better rainfall identification performance of MW techniques for monitoring purposes. The NRL algorithm or the now available TRMM 3B42RT products belong to this category. The MW pixel resolution makes a 0.25° lat-lon grid appropriate, but better spatial resolution is desired by the users.

A more comprehensive analysis of the categorical statistics of all possible combinations of the above mentioned algorithms within the period 08 to 13 Nov 2001 is given in Kästner (2003). The accuracy of all inter-comparisons is measured in terms of Heidke skill score that ranges from 0.61 (BOLAM vs. NRE), over respectable 0.78 (BOLAM vs. FDA), to optimal 0.82 comparing both PMW algorithms (PATER vs. FDA). The bias between PATER and NRL is small and again PATER performs best when compared with FDA, their bias is neglectable. Worthwhile to note that even in this heavy rain event only 10% of the gridded pixels are hits (rain/rain), whereas the majority (62%) is correct negatives (no-rain/no-rain), thus, the correct negatives dominate the statistics.

4. MONTHLY MEANS OF RAINFALL

The MW PATER algorithm over ocean by Bauer (2001) is applied to all available orbits that hit the Mediterranean region extending from 30°W to 40°E (Azore Islands to Israel) and 25°N to 40°N (Canary Islands to Sicily) in the winter rain period November 2002 till May 2003. The Mediterranean climate is characterized by winter rains and summer droughts. The strong difference between the wet winters and the dry summers is caused by the seasonal alternation of the dominance of cyclonic storms in winter and subtropical high pressure cells over the adjacent ocean in summer with subsiding maritime tropical air. Only in the European area, because of the Mediterranean Sea, the Mediterranean climate covers the wide area of 3.1 Mkm² while in most other regions it is confined to narrow coastal belts (Bolle, 2003).

Within the belt of the Mediterranean climate exists a strong gradient of the meteorological parameters, the precipitation ranges between 0 and 300 mm/month accumulated rainfall. For this study all available TRMM data of the Mediterranean belt and within one month contribute to the monthly mean RR given in mm/h. The single observation is instantaneous and some problems occur when averaging, nevertheless the gridded (0.25° lat-lon) monthly mean RR reveal some interesting features. When neglecting the averaging problems the evaluated RR can roughly be converted into accumulated rainfall by multiplication with a factor of 90, resulting from 3 orbits per day times 30 days per month, then the scale runs from 0 to 110 mm accumulated rainfall.

Figure 8 shows the geographical distribution and the temporal development in the rainy winter period 2002/2003 by selected months from November to May.

Within the Atlantic there is a west-east gradient towards the coasts of Africa and Spain, especially in January and May. Further, a gradient to the north is detectable over the Atlantic.

Over the Mediterranean Sea the high spatial variability even at relatively small scales is seen in every month. Maximum precipitation over the southern Mediterranean Sea occurred for this winter period in March 2003. The northern part of the Mediterranean Sea is outside the TRMM coverage.

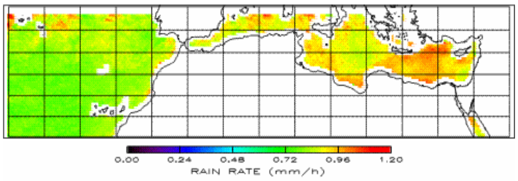

November 2002

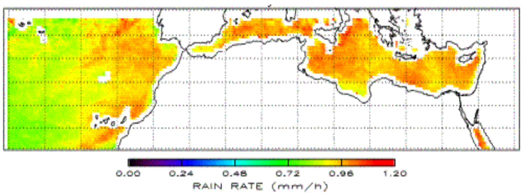

January 2003

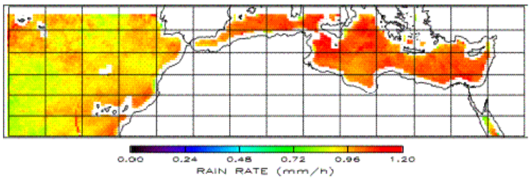

March 2003

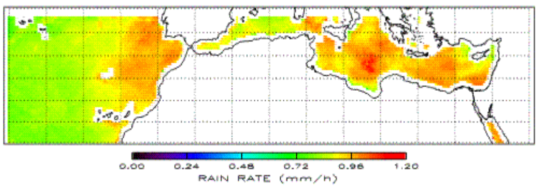

May 2003

Fig 8: Geographical distribution of precipitation in the winter season 2002/2003 using the MW satellite rain retrieval PATER (Bauer, 2001)

ACKNOWLEDGEMENT

This research is funded by the EURAINSAT project, a shared-cost project (contract EVG1-2000-00030), co-funded by the Research DG of the European Commission within the RTD activities of a generic nature of the Environment and Sustainable Development sub-programme in the 5th Framework Programme.

REFERENCES

Bauer P, Amayenc P, Kummerow CD, Smith EA, 2001: Over–Ocean Rainfall Retrieval from Multisensor Data of the Tropical Rainfall Measuring Mission. Part II: Algorithm Implementation. *J. Atmos. Oceanic Technol*., **18**, 1838-1855.

Bolle, H-J (ed.): *Mediterranean Climate – Variablility and Trends.* Berlin, Springer, 372 pp, 2003.

Buzzi A, D'Isidoro M, Davolio S, 2003: A case study of an orographic cyclone formation south of the Alps during the MAP-SOP. *Q. J. R. Meteorol. Soc.*, **129**, 1795-1818.

Grody NC, 1991: Classification of snow cover and precipitation using the Spacial Sensor Microwave/ Imager (SSM/I). J. Geophys. Res., **96**, 7423-7435.

Grose A, Smith EA, Chung H-S, Ou ML, Sohn BJ, Turk FJ, 2002: Possibilities and limitations for QPF using nowcasting methods with infrared geosynchronous satellite imagery. *J. Appl. Meteor*., **41**, 763-785.

Kästner M, 2003: Inter-comparison of precipitation estimations using TRMM microwave data and independent data. In: Proc. 3rd GPM Workshop - Consolidating the Concept, Noordwijk, The Netherlands, 24-26 June 2003, AP-5. http://www.estec.esa.nl/conferences/03C06/

Kidd C, Kniveton D, Todd M, Bellerby T, 2003: Satellite rainfall estimation using a combined passive microwave and infrared algorithm. *J. Hydrometeorology,* **4**, 1088-1104.

Kummerow C, Olsen WS, Giglio L, 1996: A simplified scheme for obtaining precipitation and vertical hydrometeor profiles from passive microwave sensors. *IEEE Trans. Geosci. Remote Sens.*, **34**, 1213-1232.

Oh HJ, Sohn BJ, Smith EA, Turk FJ, Seo AS, Chung HS, 2002: Validating infrared-based rainfall retrieval algorithms with 1-minute spatially dense raingauge measurements over the Korean peninsula. *Meteor. Atmos. Physics*, **81**, 273-287.

Thomas W, Baier F, Erbertseder T, Kästner M, 2003: Analysis of the Algerian severe weather event in November 2001 and its impact on ozone and nitrogen dioxide distributions. *Tellus B*, **55B**, 993-1006.

Turk FJ, Ebert EE, Oh HJ, Sohn BJ, Levizzani V, Smith EA, Ferraro R, 2002: Validation of an operational global precipitation analysis at short time scales. In: Proc. 1st Worskshop Intern. Precip. Working Group (IPWG), Madrid, Spain, 23-27 Sept. 2002.

Wentz FJ and Spencer RW, 1998: SSM/I rain retrievals within an unified all-weather ocean algorithm. *J. Atmos. Sci.*, **55** (9), 1613-1627.